Coordination chemistry of sulfamethizole: crystal structures of [Cu(sulfamethizolate)$_2$(py)$_2$(OH$_2$)]·H$_2$O, [M(sulfamethizolate)$_2$(py)$_2$(OH$_2$)$_2$] [M = Co and Ni] and {Cu(sulfamethizolate)$_2$(dmf)$_2$}$_\infty$

Elisa Borrás [a], Gloria Alzuet [b], Joaquín Borrás [b,*], Juan Server-Carrió [b], Alfonso Castiñeiras [c], Malva Liu-González [d], Francisco Sanz-Ruiz [d]

[a] *Departamento de Bioquímica y Biologia Molecular, Facultad de Medicina y Odontología, Universidad de Valencia, Avda. Vicente Blasco Ibáñez, 17, E-46010 Valencia, Spain*
[b] *Departamento de Química Inorgánica, Facultad de Farmacia, Universidad de Valencia, Avda. Vicent Andrés Estellés s/n, E-46100 Burjassot, Spain*
[c] *Departamento de Química Inorgánica, Facultad de Farmacia, Universidad de Santiago de Compostela, E-15703 Santiago de Compostela, Spain*
[d] *Departamento de Termología, Facultad de Fisicas, Universidad de Valencia, Dr Moliner, 50, 46100 Burjassot, Spain*

Abstract

The synthesis and characterisation of copper, cobalt, nickel and zinc compounds with sulfamethizole (4-amino-N-(5-methyl-1,3,4-thiadiazole-2-yl)sulfanilamide) (Hsmtz) are described. The first crystal structures of ternary sulfamethizole complexes are reported. The crystal structures of Cu(smtz)$_2$(py)$_2$(OH$_2$)·H$_2$O (**1**), M(smtz)$_2$(py)$_2$(OH$_2$)$_2$ [M = Co (**2**), Ni (**3**)] and {Cu(smtz)$_2$(dmf)$_2$}$_\infty$ (**5**) were determined by X-ray diffraction. The Cu(II) ion exhibits a square pyramidal geometry in complex **1**, while in the other compounds the metal ion presents a distorted octahedral environment. In compounds **1**, **2** and **3** the deprotonated sulfamethizole acts as monodentate ligand coordinating through the thiadiazole N atom and in compound **5** it behaves as a bridge linking two metal cations via the thiadiazole and the amino nitrogen atoms. The IR, electronic, EPR and thermal data are consistent with the crystal structures. © 2000 Elsevier Science Ltd. All rights reserved.

Keywords: Sulfamethizole; Metal complexes; Crystal structures; Spectroscopic properties

1. Introduction

Among the N-substituted sulfanilamides, sulfamethizole (4-amino-N-(5-methyl-1,3,4-thiadiazole-2-yl)sulfanilamide) (Hsmtz) (Scheme 1) is one of the most used antibacterial drugs. It is expended as 'thiosulfil'. Sulfamethizole is extensively used in the treatment of the urinary tract infections [1]. The mechanism of action is based on the competitive antagonism of PABA (*p*-aminobenzoic acid) and the sulfanilamide derivative. Recently, sulfamethizole has been used as capsules containing contrast medium for assessment of gastric emptying in functional dyspepsia patients [2].

The Hsmtz has several groups with donor atoms that are able to interact with metal ions. Metal complexes of Hsmtz have been reported [3], but until now no crystal structure of binary or ternary sulfamethizole metal complexes had been determined. Previously, we have undertaken an investigation on the coordination properties of the sulfathiazole [4-amino-N-2-thiazolylbenzenosulfonamide, Hstz], a sulfonamide closely related
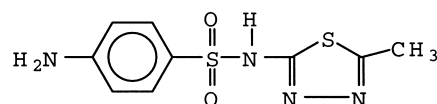
Scheme 1. 4-amino-N-(5-methyl-1,3,4-thiadiazole-2-yl)sulfanilamide (sulfamethizole).

---

* Corresponding author. Tel.: + 34-6-386-4530; fax: + 34-6-386-4960.
E-mail address: joaquin.borras@uv.es (J. Borrás).

to sulfamethizole. We have found that it presents different coordination behaviour as a ligand, acting as: (i) monodentate through the amino group [4,5]; (ii) monodentate via the thiazole N atom [6]; (iii) bidentate bridging two metal ions through the N_{amino} and the $N_{thiazole}$ [7]; (iv) bidentate through the $N_{thiazole}$ and the $N_{sulfonamido}$ [8]; (v) bidentate to one Cu(II) through the $N_{thiazole}$ and the $N_{sulfonamido}$ and bridging to an adjacent Cu(II) through the N_{amino} [9].

The different coordination abilities of the sulfathiazole have led us to study the chelating properties of the sulfamethizole in order to compare the behaviour of both sulfanilamides. In this work we synthesise and characterise Cu, Co, Ni and Zn complexes of sulfamethizole and report the first crystal structures of sulfamethizolate complexes.

2. Experimental

2.1. Physical measurements

All reagents were of the highest grade commercially available and used without further purification. Elemental analyses (C, H, N) were done at the microanalytical laboratory of the University of Salamanca. IR spectra were recorded on a Mattson Satellite FTIR spectrometer. Samples were prepared using the KBr technique. Electronic spectra were registered on a Shidmazu UV 2101PC spectrophotometer using the diffuse reflectance technique. EPR spectra were carried out with a Brucker ER 200 D spectrometer. Magnetic susceptibility measurements at r.t. were taken with a fully automatized AZTEC DSM8 pendulum-type susceptometer. Mercury tetrakis(thyocianato)cobaltate(II) was used as a susceptibility standard. Data were corrected for diamagnetic contribution, which were estimated from Pascal's constants. Thermogravimetric analyses were made in air atmosphere using a Shimadzu TGA-50H.

2.2. Synthesis of the complexes

2.2.1. Cu(smtz)$_2$(py)$_2$(OH$_2$)·H$_2$O (1)

A 50 ml sample of a 1:1 aqueous pyridine solution containing 5 mmol of Hsmtz was added to an equal volume of an aqueous solution of CuSO$_4$·5H$_2$O (10 mmol) containing 25% per volume of pyridine, slowly and with continuous stirring. Immediately, the mixture took on an intense blue colour. After 3 days prismatic blue crystals were obtained. They were filtered, washed and dried at vacuum. *Anal*. Calc. for C$_{28}$H$_{30}$N$_{10}$O$_5$S$_4$: C, 43.2; H, 3.8; N, 18.0; Cu, 8.2. Found: C, 42.4; H, 4.0; N, 17.7; Cu, 8.1%.

2.2.2. M(smtz)$_2$(py)$_2$(OH$_2$)$_2$ [M = Co (2), Ni (3), Zn (4)]

The compounds were obtained by a procedure similar to that described for the copper complex but using CoCl$_2$·6H$_2$O, NiCl$_2$·6H$_2$O and ZnCl$_2$·2H$_2$O instead of CuSO$_4$·5H$_2$O. The resulting solutions were orange, blue and white, respectively. They were left to stand at r.t. and after few days single crystals suitable for X-ray diffraction were obtained for the Co and Ni complexes, while a white solid was obtained for the Zn complex. *Anal*. Calc. for C$_{28}$H$_{32}$CoN$_{10}$O$_6$S$_4$: C, 42.5; H, 4.0; N, 17.7. Found: C, 42.8; H, 4.0; N, 17.6%. *Anal*. Calc. for C$_{28}$H$_{32}$N$_{10}$O$_6$S$_4$: C, 43.2; H, 3.8; N, 18.0. Found: C, 42.4; H, 4.0; N, 17.7%. *Anal*. Calc. for C$_{28}$H$_{32}$ZnN$_{10}$O$_6$S$_4$ C, 42.1; H, 4.0; N, 17.5. Found: C 42.6; H 3.9; N 17.8%.

2.2.3. {Cu(smtz)$_2$(dmf)$_2$}$_\infty$ (5)

Sulfamethizole (3 mmol) was added to 1 mmol of copper acetate in 30 ml of dimethylformamide. The resulting solution was left to stand at r.t. and after few days prismatic green crystals were obtained. *Anal*. Calc. for C$_{24}$H$_{32}$CuN$_{10}$O$_6$S$_4$: C, 38.5; H, 4.3; N, 18.7. Found: C, 38.9; H, 4.1; N, 18.9%.

2.3. Crystallographic data and structure determination

2.3.1. Cu(smtz)$_2$(py)$_2$(OH$_2$)·H$_2$O (1) and Ni(smtz)$_2$(py)$_2$(OH$_2$)$_2$ (3)

Diffraction measurements of the selected blue (Cu) and pale green (Ni) prismatic crystals, with approximate sizes $0.10 \times 0.20 \times 0.25$ mm (Cu) and $0.15 \times 0.25 \times 0.25$ mm (Ni), were carried out at 290 K using an Enraf–Nonius CAD-4 single-crystal diffractometer with graphite monochromated Mo Kα radiation ($\lambda = 0.7107$ Å). The unit cell dimensions were determined from the angular settings of 25 reflections with $9 < \theta < 13°$ (Cu) and $8 < \theta < 14°$ (Ni). The intensity data of 6965 (Cu) and 3281 (Ni) reflections were measured in the limits $1 < \theta < 25°$ using $\omega–2\theta$ scan technique, variable speed, width $(0.80 + 0.35\tan\theta)°$ in ω and maximum scan time of 60 s per reflection in the *hkl* ranges 0–18, 0–13, −23–23 (Cu) and 0–9, −12–12, −12–12 (Ni). Three reflections were measured every hour as intensity controls without significant decay. Some double measured reflections were averaged, $R_{int} = 0.025$ (Cu) and 0.007 (Ni), resulting in 6079 (Cu) and 2957 (Ni) independent reflections of which 3673 (Cu) and 2441 (Ni) were considered, observed with the $[I > 2\sigma(I)]$ criterion. Absorption correction was not applied. The structure was solved by direct methods using the program SIR92 [10]. All non-hydrogen atoms were anisotropically refined by least-squares on F_{obs} using the X-RAY76 System [11]. The hydrogen atoms, kept fixed in the refinement with a common isotropic thermal parameter, were located by difference synthesis. In the

Table 1
Crystal data and structure refinement for Cu(smtz)$_2$(py)$_2$(OH$_2$)·H$_2$O (**1**), M(smtz)$_2$(py)$_2$(OH$_2$)$_2$ (M = Co (**2**), Ni(**3**)) and {Cu(smtz)$_2$(dmf)$_2$}$_\infty$ (**5**)

	1	2	3	5
Formula	C$_{28}$H$_{32}$Cu-N$_{10}$O$_6$S$_4$	C$_{28}$H$_{32}$Co-N$_{10}$O$_6$S$_4$	C$_{28}$H$_{32}$N$_{10}$-NiO$_6$S$_4$	C$_{24}$H$_{32}$N$_{10}$-O$_6$S$_4$Cu
Symmetry	monoclinic	triclinic	triclinic	monoclinic
Space group	$P2_1/a$	$P\bar{1}$	$P\bar{1}$	$P2_1/c$
a (Å)	15.668(3)	8.4013(14)	8.3700(4)	9.408
b (Å)	11.279(1)	10.5612(17)	10.520(1)	14.737
c (Å)	19.559(2)	10.7828(12)	10.831(1)	11.882
α (°)	90.0	75.099(13)	75.16(1)	90.0
β (°)	90.75(1)	76.034(12)	76.01(1)	111.27
γ (°)	90.0	68.555(12)	68.48(1)	90.0
V (Å^3)	3456.2(8)	848.9(2)	846.0(1)	1535.2
Z	4	1	1	2
D_{calc} (g cm^{-3})	1.53	1.549	1.55	1.619
M	796.4	791.81	791.6	748.36
$F(000)$	1644	409	410	774
μ (cm^{-1})	9.31	8.09	8.78	10.29
Goodness-of-fit	0.85	1.044	1.24	1.0152
R	0.053	0.0330	0.046	0.0440
Rw	0.058	0.0779	0.051	0.1470

final stages an empirical weighting scheme was chosen as to give no trends in $\langle w\Delta^2 F\rangle$ versus $\langle F_o\rangle$ and versus $\langle \mathrm{sen}\, \theta/\lambda\rangle$ using the program PESOS [12]. Geometrical calculations were made with PARST [13]. Atomic scattering factors and anomalous dispersion corrections were taken from reference [14]. All calculations were performed on a VAX6410. Graphical manipulations were produced by the ORTEP-3 for Windows program [15]. Other relevant parameters of the crystal structure determination are listed in Table 1.

2.3.2. Co(smtz)$_2$(py)$_2$(OH$_2$)$_2$ (2)

A rose-coloured prismatic crystal of Co(smtz)$_2$(py)$_2$-(H$_2$O)$_2$ was mounted on a glass fibre and used for data collection. Cell constants and an orientation matrix for data collection were obtained by least-squares refinement of the diffraction data from 25 reflections in the range of $11.00 < \theta < 18.12°$ in an Enraf–Nonius MACH3 automatic diffractometer [16]. Data were collected at 293 K using Mo Kα radiation ($\lambda = 0.71073$ Å) and the ω-scan technique, and corrected for Lorentz and polarisation effects [17]. A semi-empirical absorption correction (ψ-scans) was made [18]. The structure was solved by direct methods [19] and subsequent difference Fourier maps, and refined on F^2 by a full-matrix least-squares procedure using anisotropic displacement parameters [20]. All hydrogen atoms were located from difference Fourier maps and were refined isotropically. Atomic scattering factors from International Tables for X-ray Crystallography [14]. Molecular

graphics from PLATON-98 [21]. A summary of the crystal data, experimental details and refinement results are listed in Table 1.

2.3.3. {Cu(smtz)$_2$(dmf)$_2$}$_\infty$ (5)

A green crystal, size $0.2 \times 0.2 \times 0.2$ mm was mounted on an Enraf–Nonius CAD-4 single-crystal diffractometer with graphite monochromated Mo Kα radiation ($\lambda = 0.7173$ Å). The unit cell dimensions were determined from the angular settings of 25 reflections with $3.57 < \theta < 25.98°$. The space group was determined to be $P2_1/c$ from systematic absences. The intensity data of 3025 reflections, in the *hkl* range $(0, 0, -14)$ to $(11, 18, 13)$ and limits $(0 < \theta < 25°)$ were measured using the $\omega-2\theta$ scan technique and variable scan rate with a maximum scan time of 60 s per reflection. The intensity of the primary beam was checked throughout the data collection by monitoring three standard reflections every 60 min. On all reflections profile analysis was performed [22]. Lorentz-polarization corrections were applied and then the data were reduced to F_o^2 values. The structure was solved by Patterson methods using DIRDIF [23]. Isotropic least squares refinement on F^2 was made using SHELX-93[24]. During the final stages of the refinement on F^2 the positional parameters and the anisotropic thermal parameters of the non-H atoms were refined. All non-hydrogen atoms were anisotropically refined. All hydrogen atoms were geometrically placed and isotropically refined. The final conventional agreement factors were $R = 0.044$ and $wR_2 = 0.147$ for 3016 observed reflections and 236 variables. The function minimised was $\Sigma w(F_o^2 - F_c^2)/\Sigma wF_o^2]^{1/2}$, $w = 1/[\sigma 2(F_o^2 + 0.0828P)^2]$ with σF_o^2 from counting statistic and $P = (\max(F_o^2) + 2F_c^2)/3$. The final difference Fourier map showed a peak of 0.54 Å^3 very close to the C11′, the others peak no deeper than -0.39 Å^3. Atomic scattering factors were taken from International Tables for X-ray Crystallography [14]. Geometrical calculations were made with PARST [13]. Graphical manipulations were performed with EUCLID [25]. All calculations were made at the University of Valencia on the S.C.S.I.E. X-ray section VAX-computers. Other relevant parameters are collected in Table 1.

3. Results and discussion

3.1. Crystal structures of Cu(smtz)$_2$(py)$_2$(OH$_2$)·H$_2$O (1), Co(smtz)$_2$(py)$_2$(OH$_2$)$_2$·(2) and Ni(smtz)$_2$(py)$_2$(OH$_2$)$_2$ (3)

Selected bond distances and angles of the three crystal structures are shown in Table 2. Figs. 1–3 show ORTEP drawings of compounds **1**, **2** and **3**, respectively.

In compound **1** the copper atom is five co-ordinated with a geometry near to a regular square pyramidal.

Table 2
Selected bond distances (Å) and angles (°) for compounds $Cu(smtz)_2(py)_2(OH_2) \cdot H_2O$ (**1**) and $M(smtz)_2(py)_2(OH_2)_2$ (M = Co (**2**), Ni (**3**))

| **1**		**2**		**3**	
Cu–O(3)	2.183(4)	Co–O(3)	2.0457(18)	Ni–O(3)	2.040(2)
Cu–N(11)	2.002(4)	Co–N(1)	2.2110(18)	Ni–N(1)	2.163(2)
Cu–N(12)	2.001(5)	Co–N(11)	2.157(2)	Ni–N(11)	2.100(3)
Cu–N(111)	2.045(5)				
Cu–N(112)	2.046(5)				
O(3)–Cu–N(11)	95.7(2)	O(3)1–Co–N(1)	90.61(7)	O(3)–Ni–N(1)	90.7(1)
O(3)–Cu–N(111)	97.9(2)				
O(3)–Cu–N(12)	97.8(2)	O(3)–Co–N(11)	90.44(8)	O(3)–Ni–N(11)	90.7(1)
O(3)–Cu–N(112)	91.4(2)				
N(11)–Cu–N(111)	88.4(2)	N(1)–Co–N(11)	90.25(7)	N(1)–Ni–N(11)	89.6(1)
N(11)–Cu–N(12)	166.5(2)				
N(11)–Cu–N(112)	90.6(2)				
N(111)–Cu–N(12)	88.4(2)				
N(111)–Cu–N(112)	170.7(2)				
N(12)–Cu–N(112)	90.4(2)				

The equatorial plane is defined by two thiadiazole N atoms from two sulfamethizolate ligands in *trans* position and by two pyridine N atoms. The axial site is occupied by a water O atom at longer distance, 2.183(4) Å. The Cu–$N_{thiadiazole}$ bond length 2.002(4) Å, is significantly shorter than the Cu–$N_{thiadiazole}$ of the related [Cu(Hacm)$_2$(tn)$_2$] compound (H$_2$acm = acetazolamide, tn = propylenediamine) [26]. The Cu–N_{py}, 2.045(5) Å ones are comparable to those found in other pyridine compounds [6]. The *cis* angles in the equatorial plane ranging from 90.6(2) to 88.4(2)° do not deviate significantly from 90°. The τ value of 0.07 [$\tau = (\alpha - \beta /60)$] indicates a small distortion from a regular square pyramidal geometry [27].

The Co(II) ion in compound **2** and the Ni(II) ion in compound **3** are six co-ordinated by two pyridine N atoms and two thiadiazole N pertaining to two sulfamethizolate ligands in the equatorial sites and two water O atoms are in the apical positions. In both complexes the M–$N_{thiadiazole}$ and the M–N_{py} are markedly longer than the M–O_w distance. So, the geometry of the complexes can be described as compressed distorted octahedral. As expected from the ionic radii of the divalent metal ions the Co–$N_{thiadiazole}$, 2.2110(18) Å and the Co–N_{py}, 2.157(2) Å are longer than the Ni–$N_{thiadiazole}$, 2.163(2) Å and the Ni–N_{py}, 2.100(3) Å. However, the corresponding M–O_w are practically the same [Co–O_w, 2.0457(18) Å and Ni–O_w, 2.040(2) Å]. The Ni–$N_{thiadiazole}$ bond is slightly longer than the same distance in the [Ni(Hacm)$_2$(NH$_3$)$_4$] complex [28]. The M–N_{py} are similar to those of the M(macm)$_2$(py)$_2$(OH$_2$)$_2$ (M = Co, Ni; macm = methazolamidate) [29]. Angles around the metal do not differ significantly from those of a regular octahedron.

Several interesting aspects can be deduced from a comparison of bond distances of the **2** and **3** complexes with those of the compound **1**. The equatorial Cu–N lengths are significantly shorter than the Co–N and the Ni–N ones. In particular, the M–$N_{thiadiazole}$ is the short-

Fig. 1. ORTEP drawing of $Cu(smtz)_2(py)_2(OH_2) \cdot H_2O$ (**1**).
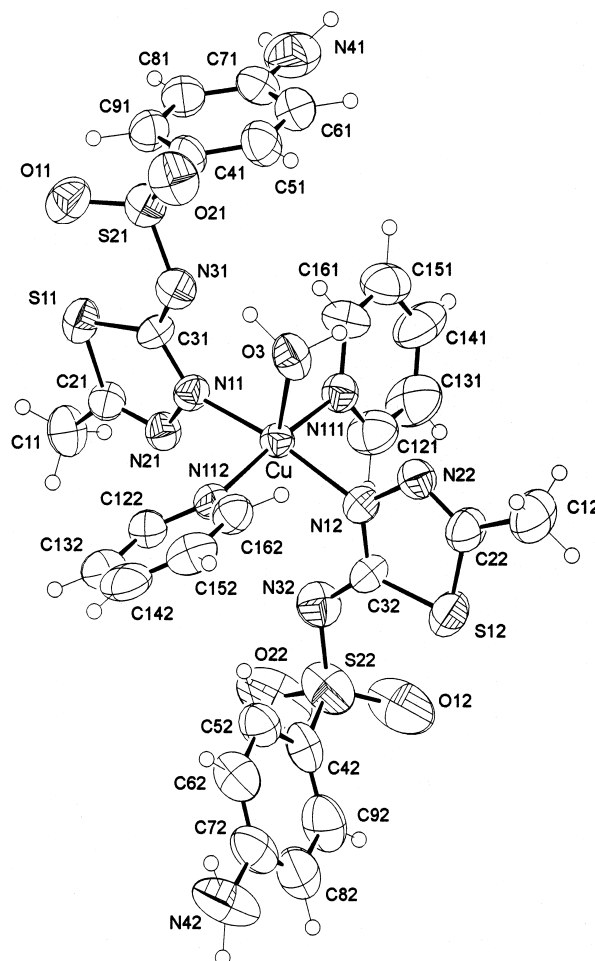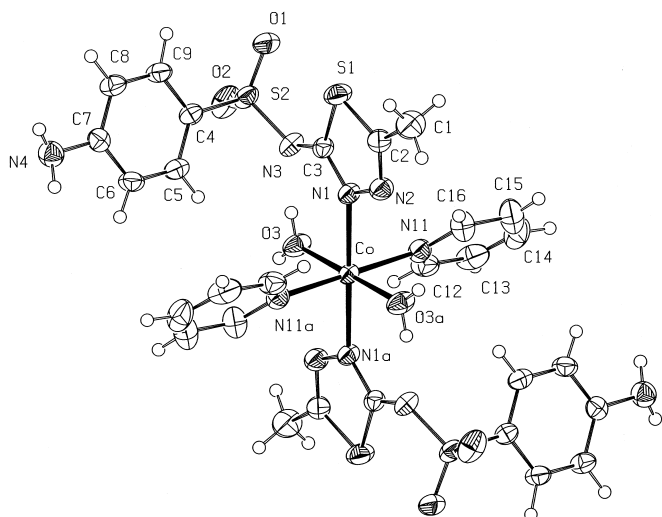
Fig. 2. ORTEP drawing of Co(smtz)$_2$(py)$_2$(OH$_2$)$_2$ (**2**).
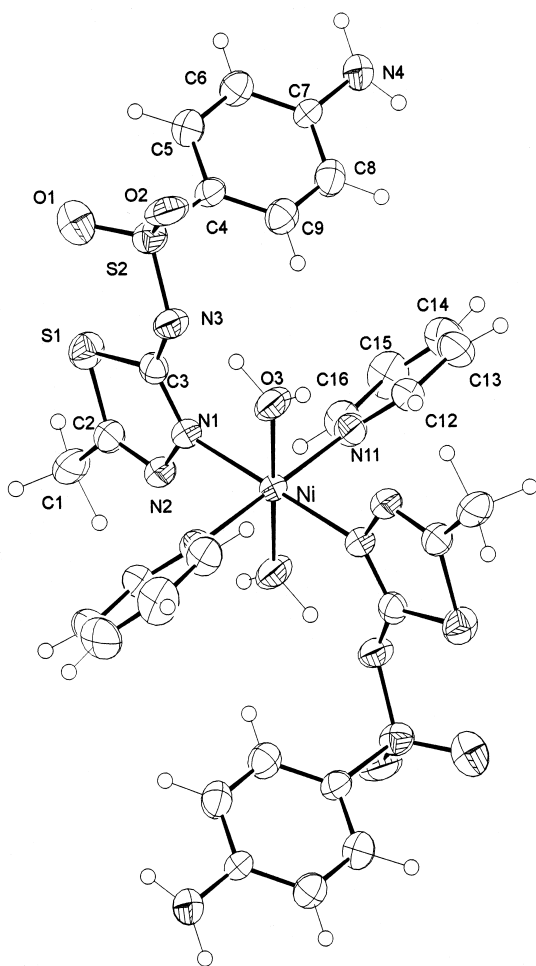
Fig. 3. ORTEP drawing of Ni(smtz)$_2$(py)$_2$(OH$_2$)$_2$ (**3**).

est bond distance in the copper complex, whereas it is the longest one in the nickel and cobalt compounds.

It must be noted that the sulfamethizole ligand acts as monodentate coordinating through the thiadiazole N

atom closest to the deprotonated sulfonamido group although it presents several donor atoms and therefore it offers different coordination possibilities. The same coordination behaviour has been exhibited by the related acetazolamide in the octahedral [Cu(Hacm)$_2$(tn)$_2$] and [Ni(Hacm)$_2$(NH$_3$)$_4$] complexes [26,28] and by the sulfathiazole in the [Cu(stz)(py)$_3$Cl] and [Cu(stz)$_2$-(mim)$_2$]·H$_2$O compounds [6,9].

3.2. Crystal structure of {Cu(smtz)$_2$(dmf)$_2$}$_\infty$ (**5**)

A drawing of the complex is presented in Fig. 4. Selected bond and angles of the coordination polyhedron are listed in Table 3.

The structure is a coordination polymer in which each Cu(II) ion presents an octahedral geometry. The equatorial plane is defined by two N$_{\text{thiadiazole}}$ atoms *trans* one another and two N$_{\text{amino}}$ atoms from four sulfamethizolate ligands. Two O atoms of two disordered dimethylformamide molecules are placed in the apical positions at the distance of 2.391(4) Å. Each cupric ion is connected with the other Cu ions by four sulfamethizolate anions acting as bridges via the N$_{\text{thiadiazole}}$ and N$_{\text{amino}}$ atoms.

The four in-plane Cu–N bond distances [Cu–N$_{\text{thiadiazole}}$, 2.083(4); Cu–N$_{\text{amino}}$, 2.056(4) Å] are similar. The Cu–N$_{\text{thiadiazole}}$ is longer than this distance in compound **1**. Regarding to the Cu–N$_{\text{amino}}$ length it is in the range found for the corresponding distances in Cu complexes of the sulfathiazole ligand [from 2.020 to 2.071 Å] [4]. The Cu–O$_{\text{dmf}}$ bond lengths can be regarded as normal [30].

The largest deviation from a regular octahedral geometry is found in the axial angles involving the amino N atoms [94.8(2) and 85.2(2)°].

The sulfamethizolate anion behaves as a bridging ligand through the N$_{\text{thiadiazole}}$ and N$_{\text{amino}}$ atoms. This coordination behaviour is different to that exhibit by the ligand in the complexes described above, although is similar to that observed for the sulfathiazole in the [Zn(stz)$_2$]·H$_2$O complex [7].

A comparison of the four crystal structures described in this paper shows that no remarks can be noted as far as the sulfamethizole bond distances are concerned. From a different coordination behaviour of the sulfamethizole in compound **5** with respect to complexes **1**, **2** and **3**, only a slight difference can be observed in the N(4)–C(7) bond lengths [1.424(6) compound **5**, 1.382(9) compound **1**, 1.398(3) complex **2** and 1.402(5) Å complex **3**]. Moreover, the different strength binding of the N$_{\text{thiadiazole}}$ does not modify significantly the N–N distance [1.390(5) compound **5**, 1.376(9) compound **1**, 1.387(3) complex **2** and 1.386(3) Å complex **3**]. This fact could be related to the charge delocalization through the thiadiazole ring as a consequence of the deprotonation of the sulfonamide group.
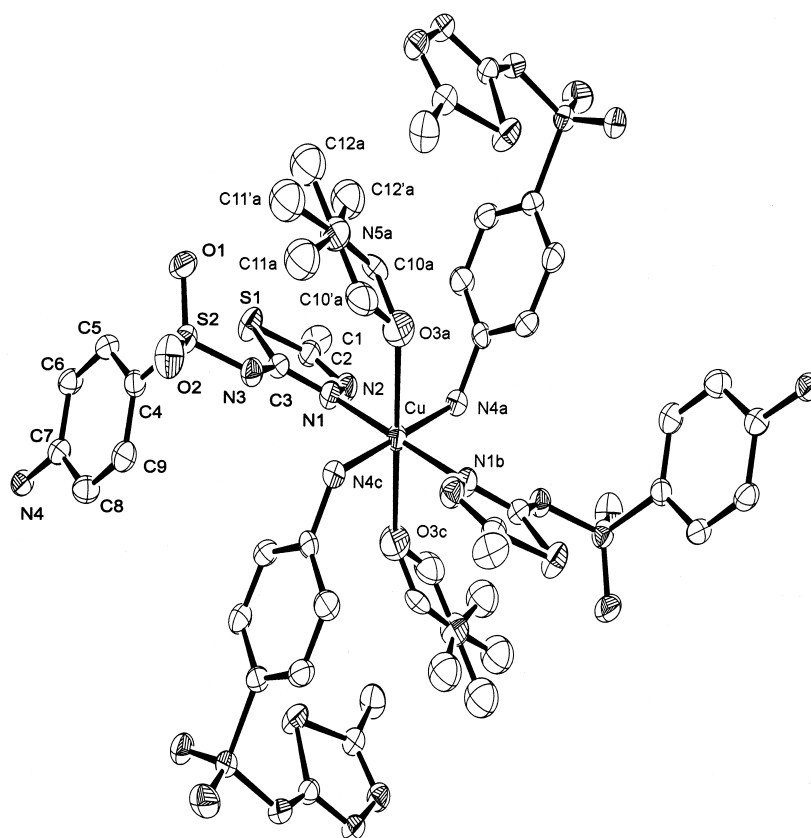
Fig. 4. ORTEP drawing of {Cu(smtz)$_2$(dmf)$_2$}$_\infty$ (**5**).

3.3. IR spectra

A comparative study of the IR spectra of the complexes with that of the free ligand and those of the complexes of related ligands gives some positive information regarding the binding sites of the sulfamethizole. All the complexes show very similar spectral pattern. The strong bands at 3440, 3360 and 3250 cm^{-1} in the IR of the ligand attributed to v_{as}(NH$_2$), v_s(NH$_2$) and v(NH) of the amino group appear at the same range in the IR spectra of complexes **1**, **2**, **3** and **4**. However, these bands are modified in the IR spectrum of the compound **5** as a consequence of the interaction of the amino group with the copper(II) ion.

With respect to the 1,3,4-thiadiazole ring modes, because of the rigidity of the penta-atomic ring, the vibrational spectra can not be interpreted in terms of localised vibrations, being many atoms involved in several vibration modes. The strong band at 1550 cm^{-1} in the ligand is shifted to 1450–1440 cm^{-1} in the complexes. On the one hand this is due to deprotonation of the sulfonamido group that gives rise to a delocalization of the negative charge between the N$_{sulfonamidate}$ and the thiadiazole ring and on the other hand, to the interaction of the N$_{thiadiazole}$ with the metal ions.

The SO$_2$ group modes of the ligand appear as strong bands at 1325 (v_{as}) and 1128 cm^{-1} (v_s). In the complexes, the asymmetric mode is shifted to 1290–1260 cm^{-1} and the symmetric vibration gives rise a band practically unchanged with respect to that of the ligand.

Table 3
Selected bond distances (Å) and angles (°) for {Cu(smtz)$_2$(dmf)$_2$}$_\infty$ (**5**) [a]

Cu–O(3) # 1	2.391(4)
Cu(1)–O(3) # 2	2.391(4)
Cu–N(1)	2.083(4)
Cu(1)–N(1) # 3	2.083(4)
Cu–N(4) # 1	2.056(4)
Cu(1)–N(4) # 2	2.056(4)
O(3) # 1–Cu–O(3) # 2	180.0
N(4) # 1–Cu–N(1)	88.4(2)
N(4) # 2–Cu–N(1)	91.6(2)
N(4) # 1–Cu–N(4) # 2	180.0
N(4) # 1–Cu–O(3) # 1	94.8(2)
N(4) # 2–Cu–O(3) # 1	85.2(2)
N(1)–Cu–O(3) # 1	89.2(2)
N(1) # 1–Cu–O(3) # 1	90.8(2)
N(1)–Cu–N(1) # 3	180.0

[a] Symmetry transformations used to generate equivalent atoms # 1: $-x+2$, $y-1/2$, $-z+5/2$; # 2: x, $-y+1/2$, $z-1/2$; # 3 $-x+2$, $-y$, $-z+2$; # 4: $-x+2$, $y+1/2$, $-z+5/2$.

In spite of the coordination of one of the $N_{thiadiazole}$ to metal ions, the complexes present the same N–N bond distances so, the band located at 990 cm^{-1} assigned to a v(N–N) mode does not change in the IR spectra of the complexes.

A shift of the v(S–N) band is observed in the IR spectra of the complexes (940–930 cm^{-1}) with respect to that of the ligand (920 cm^{-1}). This could be attributed to deprotonation of the sulfonamido group and consequently the shortening of the S–N bond distance.

A band at 3470 cm^{-1} in the IR spectra of the compounds **1** and **4** is attributed to v(O–H) vibration. The IR spectrum of the complex **5** shows a strong band at 1650 cm^{-1} assigned to a v(C=O) vibration of the dmf molecules. The pyridine ring breathing band in compounds **1**, **2**, **3** and **4** is found at 1040 cm^{-1}, according to the fact that the pyridine molecules are coordinated [31].

3.4. Magnetic properties, electronic and EPR spectra

At room temperature the Cu(II) complexes have magnetic moment (2.01 BM for **1** and 1.94 BM for **5**) somewhat higher than the spin-only value. Such divergence is not uncommon in mononuclear Cu(II) complexes due to mixing-in of some angular momentum from the closely lying excited states via spin–orbit coupling [32]. The cobalt complex presents a magnetic moment (4.11 BM) slightly lower than the common values of octahedral complexes. This fact could be attributed to the distortion of the coordination polyhedra that leads to a minor orbital contribution to the magnetic moment. The magnetic moment value for the Ni(II) compound (2.90 BM), indicative of a slight orbital contribution, is in the range found for octahedral complexes.

The diffuse reflectance (DR) spectra of the Cu(smtz)$_2$(py)$_2$(OH$_2$)·H$_2$O (**1**) and the {Cu(smtz)$_2$(dmf)$_2$}$_\infty$ (**5**) with a well-defined d–d maximum at 595 (compound **1**) and 660 nm (compound **5**) agree well with the square pyramidal geometry and the octahedral geometry deduced from their crystal structures. The DR spectra of compounds **2** and **3** (with maxima at 490 and 600 nm, respectively) fit for an octahedral environment according to their crystal structures.

Intense absorption in the ultraviolet region (ca. 300 nm) is a feature common to all the complexes and it is attributed to an intra-ligand transition.

The polycrystalline powder EPR spectrum at room temperature of the compound **1** is axial in nature with a poorly resolved parallel component. The EPR spectrum of the zinc copper-doped compound is also axial anisotropy with a four-line hyperfine structure due to the interaction of the unpaired electron with the nuclear spin of the copper nucleus. The ground state parameters extracted from the experimental spectrum by simulation [33], $g_{\|} = 2.26$, $g_{\perp} = 2.07$ and $A_{\|} = 140 \times 10^4$ cm^{-1} are in good agreement with a square pyramidal geometry. The compound **5** shows a rhombic polycrystalline powder EPR spectrum with $g_3 = 2.20$; $g_2 = 2.13$ and $g_1 = 2.08$ values, according to the copper coordination polyhedron.

3.5. Thermal analyses of compounds 1–4

The thermal study of the compound **1** has a first step at 120°C corresponding to the loss of two water molecules (% experimental weight 4.78; calculated weight 4.52). The second step, that take place at 180°C, corresponds to a loss of the two pyridine molecules (% experimental weight 17.94; calculated weight 19.86). There is a third step at 350°C where the two aniline groups of the sulfonamidate are lost (% experimental weight 25.62, calculated 23.38) and a fourth step where the pyrolytic decomposition takes place leaving a percentage residual weight of 12.85% that can be attributed to a mixture of CuO and CuSO$_4$.

The compound **2** is stable to 110–120°C. At this temperature range the first step of the thermal decomposition starts. This step corresponds to the loss of the two pyridine ligands (% experimental weight 19.06, calculated weight for two pyridines 19.98). Between 200–250°C a second step occurs where the weight loss corresponds to a water molecules and aniline groups of the sulfonamidate ligand (% experimental weight 34.25, calculated weight 31.62). In a third step the pyrolytic decomposition of the rest takes place, yielding a residue that it is a mixture of cobalt sulphate and cobalt oxide.

The TG curve of the compound **3** presents a first step (150°C) where the loss of the pyridine and water molecules takes place at the same time (% experimental weight 23.07. calculated weight 24.54). The second (250–500°C) and third (500–600°C) steps agree with the pyrolytic decomposition of the compound. As in the other processes the residue is a mixture of nickel sulphate and nickel oxide.

The TG curve of the compound **4** shows two separate thermal events. Until 150°C the compound does not present any loss of weight. Between 150–400°C a first step takes place with a weight loss of 52.68% that can be attributed to a loss of two pyridine, two water molecules and two aniline groups. The second step corresponds to the pyrolytic decomposition of the compound. The residue is composed of a mixture of zinc sulphate and zinc oxide.

From a comparison of the first step of the thermal process we can observe a different stability of the water molecules between the compound **1** and the rest of the complexes. The lower temperature of water loss in the compound **1** can be related with the larger Cu–OH$_2$ bond length observed in this compound with respect to

the other M–OH$_2$ bond distances (M = Co and Ni) in the compounds **2** and **3**.

4. Supplementary data

Supplementary crystallographic data have been deposited with the Cambridge Crystallographic Data Centre, CCDC Nos. 140608, 140609, 140610 and 140611. Copies of this information may be obtained free of charge from The Director, CCDC, 12 Union Road, Cambridge, CB2 1EZ, UK (fax: + 44-1223-336-033; e-mail: deposit@ccdc.cam.ac.uk or www: http://www.ccdc.cam.ac.uk).

References

[1] E.R. Barnhart (Ed.), Physician's Desk Reference, PDR, 43rd ed., Medical Economics, New York, 1989.

[2] T. Suzuki, Y. Yamamoto, K Abe, M. Hirano, H. Oka, Dig. Dis. Sci. 44 (1999) 1741.

[3] A. Bult, Metal complexes of sulfanilamides, in: Metal Ions in Biological Systems, Sigel ed., Marcel Dekker, New York, 1983.

[4] J. Casanova, G. Alzuet, J. Borrás, J. Timoneda, S. García-Granda, I. Cándano-González, J. Inorg. Biochem 56 (1994) 65.

[5] J. Casanova, G. Alzuet, J. Borrás, J.M. Amigó, T. Debaerde-maeker, Z. Kristallogr. 209 (1994) 271.

[6] J. Casanova, G. Alzuet, J. Borrás, J. Latorre, M. Sanaú, S. García-Granda, J. Inorg. Biochem 60 (1995) 219.

[7] J. Casanova, G. Alzuet, S. Ferrer, J. Borrás, J. Timoneda, S. García-Granda, E. Pérez-Carreño, J. Inorg. Biochem. 51 (1993) 689.

[8] J. Casanova, G. Alzuet, J. Latorre, J. Borrás, Inorg. Chem. 36 (1997) 2052.

[9] J. Casanova, G. Alzuet, J. Borrás, O. Carugo, J. Chem. Soc., Dalton Trans. (1996) 2239.

[10] A. Altomare, M.C. Burla, M. Camalli, G. Cascarano, G. Giacovazzo, A. Guagliardi, G. Polidori, J. Appl. Crystallogr. 27 (1994) 435.

[11] J.M. Stewart, P.A. Machin, C.W. Dickinson, H.L. Ammon, H. Heck, H. Flack, The X-RAY76 system, in: Technical Report TR-446, Computer Science Center, University of Maryland, College Park, MD, 1976.

[12] Martínez-Ripoll, M. Cano, F.H. PESOS Computer Program, Instituto Rocasolano, C.S.I.C., Madrid, Spain, 1975.

[13] M. Nardelli, Comput. Chem. 7 (1983) 95.

[14] International Tables for X-ray Crystallography, vol. 4, Kynoch Press, Birmingham, 1974, p. 71–79, 149.

[15] L.J. Farrugia, J. Appl. Crystallogr. 30 (1997) 565.

[16] B.V. Nonius, CAD4-Express Software, Ver. 5.1/1.2. Enraf Nonius, Delft, The Netherlands, 1994.

[17] M. Kretschmar, GENHKL Program for the Reduction of CAD4 Diffractometer Data, University of Tübingen, Germany, 1997.

[18] A.C.T. North, D.C. Phillips, F.S. Mathews, Acta Crystallogr., Sect. A 24 (1968) 351.

[19] G.M. Sheldrick, Acta Crystallogr., Sect. A 46 (1990) 467.

[20] G.M. Sheldrick, SHELXL-97, Program for the Refinement of Crystal Structures, University of Göttingen, Germany, 1997.

[21] A.L. Spek, PLATON, A Multipurpose Crystallographic Tool, Utrecht University, Utrecht, The Netherlands, 1999.

[22] M.S. Lehman, F.K. Larsen, Acta Crystallogr., Sect. A 30 (1974) 580.

[23] P.T. Beurskens, P.T. Admiraall, G. Beurskens, W.P. Bosman, S. García-Granda, R.O. Gould, J. M.M. Smits, C. Smykalla, DIRDIF User's Guide Technical Report, Crystallography Laboratory, University of Nijmegen, The Netherlands, 1992.

[24] G.M. Sheldrick, in: H.D. Flack, P. Parkanyi, K. Simon (Eds.), SHELX-93, Crystallographic Computing 6deIUCr, Oxford University Press, Oxford, 1993.

[25] A.L. Speck, in: D. Sayre (Ed.), The EUCLID Package, Computational Crystallography, Claredon, Oxford, 1999, p. 528.

[26] S. Ferrer, J.G. Haasnoot, R.A.G. de Graaff, J. Reedijk, J. Borrás, Inorg. Chim. Acta 192 (1992) 129.

[27] A.W. Addison, T.N. Rao, J. Reedijk, J. van Rijn, G.C. Verschoor, J. Chem. Soc., Dalton. Trans. (1984) 1349.

[28] S. Ferrer, J. Borrás, C. Miratvilles, A. Fuertes, Inorg. Chem. 28 (1989) 160.

[29] G. Alzuet, S. Ferrer, J. Borrás, A. Castiñeiras, X. Solans, M. Font-Bardía, Polyhedron 11 (1992) 2849.

[30] E. Müller, G. Bernardinelli, J. Reedijk, Inorg. Chem. 34 (1995) 5979.

[31] A.R. Katritzky, A.R. Hands, J. Chem. Soc. (1958) 2202.

[32] B.N. Figgis, J. Lewis, in: J. Lewis, R.G. Wilkins (Eds.), Modern Coordination Chemistry: Principles and Methods, Interscience, New York, 1960, p. 400.

[33] WINEPR-SimFonia. I.25, Bruker Analytik GmbH, Karlsruhe, Germany, 1994–1996.